

Successive opening of the Fermi surface in doped N -leg Hubbard ladders

Urs Ledermann, Karyn Le Hur, and T.M. Rice

Theoretische Physik, Eidgenössische Technische Hochschule, CH-8093 Zürich, Switzerland

(December 2, 2024)

We study the effect of doping away from half-filling in weakly (but finitely) interacting N -leg Hubbard ladders using renormalization group and bosonization techniques. For a small on-site repulsion U , the N -leg Hubbard ladders are equivalent to a N -band model, where at half-filling the Fermi velocities are $v_1 = v_N < v_2 = v_{N-1} < \dots$. We then obtain a hierarchy of energy-scales, where the band pairs $(j, N+1-j)$ are successively frozen out. The low-energy Hamiltonian is then the sum of $N/2$ (or $(N-1)/2$ for N odd) two-leg ladder Hamiltonians without gapless excitations (plus a single chain for N odd with one gapless spin mode) — similar to the N -leg Heisenberg spin-ladders. The energy-scales lead to a hierarchy of gaps. Upon doping away from half-filling, the holes enter first the band(s) with the smallest gap: For odd N , the holes enter first the nonbonding band $(N+1)/2$ and the phase is a Luttinger liquid, while for even N , the holes enter first the band pair $(N/2, N/2+1)$ and the phase is a Luther-Emery liquid, similar to numerical treatments of the t - J model, i.e., at and close to half-filling, the phases of the Hubbard ladders for small and large U are the same. For increasing doping, hole-pairs subsequently enter at critical dopings the other band pairs $(j, N+1-j)$ (accompanied by a diverging compressibility): The Fermi surface is successively opened by doping, starting near the wave vector $(\pi/2, \pi/2)$. Explicit calculations are given for the cases $N = 3, 4$.

PACS number(s): 71.10.Pm

I. INTRODUCTION

Interest in the field of ladder systems grew rapidly, when the possibility of superconductivity in doped two-leg ladder materials was proposed [1,2]. Experimentally, such a behavior may has been observed in a two-leg ladder material under high pressure [3]. The N -leg ladders have then been studied both as a first step towards the two-dimensional (2D) case [4] and because of their unusual physical properties. For example, spin-ladders exhibit an odd-even effect [5]; while even-leg ladders have a spin-gap, odd-leg ladders have one gapless spin mode. Similarly, the behavior upon doping is very different. The two-leg ladder is a Luther-Emery liquid, but the lightly doped three-leg ladder consists of a Luttinger liquid (LL) plus an insulating spin liquid (ISL) [6,7]. The latter is due to a truncation of the Fermi surface (FS) in two channels. Such a truncation is argued to take place also in the 2D case, where upon doping some parts of the FS become conducting and other parts remain an ISL [8].

Analytic works for (doped) ladders are usually based on the Hubbard model and restricted to a weak on-site repulsion U . Insulating behavior at half-filling is then due to umklapp processes. The two-leg ladder has been investigated by many authors over the past few years [9–12]. We note that in the lightly doped two-leg ladder paired holes form a dilute gas of hard-core bosons, which are equivalent to spinless fermions [10,12]. Away from half filling, the phases of the weak interaction limit $U \rightarrow 0$ of the three- and four-leg ladder have been derived in Refs. [13,14]. For the three-leg ladder, a C2S1 phase has been obtained upon doping (a phase with n gapless

charge- and m gapless spin modes is denoted by CnSm). This contrasts numerical findings for the (strongly interacting) t - J model, where at low dopings the phase is C1S1 [6,7]. An idea to explain this discrepancy has been given in a related context, where a one-dimensional electron gas (1DEG) was coupled to an insulating “environment” (another 1DEG) [15].

In this paper, we study the doping δ away from half-filling of N -leg Hubbard ladders in the case of weak but *finite* repulsive interactions, $0 < U \ll t_\perp, t$ (t and t_\perp denote the hopping matrix elements along- and between the chains). Previous works have taken the limit $U \rightarrow 0$ first, keeping the doping δ finite [14]. Here, we treat the opposite limit, i.e., we keep U finite and then investigate the lightly doped case $\delta \rightarrow 0$, where the umklapp interactions present at half-filling cannot be neglected. It is then advantageous to take the half-filled N -leg ladders as a starting point. For a small U , the Hubbard-model reduces to a weakly interacting N -band model. After linearization around the Fermi points, each band is characterized by a Fermi velocity v_j , where at half-filling $v_1 = v_N < v_2 = v_{N-1} < \dots$. We then obtain a *hierarchy of energy-scales* $T_j \sim t e^{-\alpha v_j/U}$ (α is a constant of the order of 1), where the band pairs $(j, N+1-j)$ scale towards a two-leg ladder fixed point and become successively frozen out. In particular, for N even, all excitations are gapped. For odd N , the remaining band behaves like a single chain such that the charge degrees of freedom acquire a gap while the spin-excitations stay gapless. We therefore recover the odd-even effect that is present in Heisenberg spin-ladders.

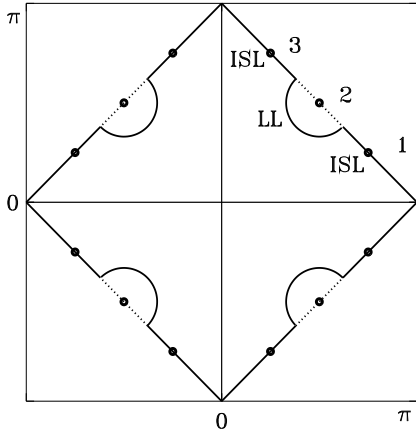


FIG. 1. The bands of the three-leg ladder correspond to three different points on a 2D FS (denoted by 1, 2, and 3). The square is the umklapp surface, which is the FS at half-filling (for $t = t_{\perp}$). The half-circles indicate the opening of the FS, when the band two is doped. At (close to) the wave vector $(\pi/2, \pi/2)$, the phase is then a LL, while at $(3\pi/4, \pi/4)$ and $(\pi/4, 3\pi/4)$, the phase is an ISL.

The gaps for the band pairs are given by $\Delta_j \sim T_j$ resulting in a *hierarchy of gaps*. Upon doping, the holes enter first the band(s) with the smallest gap. For odd N , the gap of the single chain is the smallest one and at lowest doping, the phase is a LL (C1S1). For even N , the spin degrees of freedom remain gapped upon doping and the phase is a Luther-Emery liquid (C1S0). These phases are the same as obtained in numerical treatments of the strongly interacting t - J model [4,6,7,16], i.e., at and close to half-filling, the phases for small and large U are the same. For increasing doping, paired holes enter at critical dopings, where each time the compressibility diverges, subsequently the other band pairs ($j, N+1-j$). In other words, the FS is *successively* opened, first near the wave vector $(\pi/2, \pi/2)$, spreading towards the wave vectors $(\pi, 0)$ and $(0, \pi)$ for increasing doping, see Figs. 1 and 2. Explicit calculations will be given for the cases $N = 3, 4$. The low-energy physics is derived by a combination of the renormalization group (RG) [17] and bosonization methods [18,19].

In Sec. II, the N -leg Hubbard model is introduced and the phases at half-filling are derived. In Sec. III, we study the doping away from half-filling; first for the case when only one band (pair) is doped and then for increasing doping when many band pairs become doped.

II. HALF FILLED N -LEG HUBBARD LADDERS

A. The Hamiltonian

The N -leg Hubbard model is given by $H = H_0 + H_{\text{Int}}$, where the kinetic energy is

$$H_0 = -t \sum_{x,j,s} d_{js}^{\dagger}(x+1) d_{js}(x) + \text{H.c.} \\ -t_{\perp} \sum_{x,j,s} d_{j+1s}^{\dagger}(x) d_{js}(x) + \text{H.c.} \quad (1)$$

and the interaction term is

$$H_{\text{Int}} = U \sum_{j,x} d_{j\uparrow}^{\dagger}(x) d_{j\uparrow}(x) d_{j\downarrow}^{\dagger}(x) d_{j\downarrow}(x). \quad (2)$$

The hopping matrix elements along- and perpendicular to the legs are denoted by t and t_{\perp} respectively and $U > 0$ is the on-site repulsion. For weak interactions, $U \ll t_{\perp}, t$, it is advantageous first to diagonalize H_0 ,

$$H_0 = \sum_{j,s} \int dk \epsilon_j(k) \Psi_{js}^{\dagger}(k) \Psi_{js}(k), \quad (3)$$

where Ψ_{js}^{\dagger} and Ψ_{js} are the creation- and annihilation operators for the band j . For open boundary conditions perpendicular to the legs, the dispersion relations ϵ_j are given by ($j = 1, \dots, N$)

$$\epsilon_j(k) = -2t \cos(k) - 2t_{\perp} \cos[\pi j/(N+1)]. \quad (4)$$

The Fermi momenta in each band k_{Fj} are determined by the chemical potential $\mu = \epsilon_j(k_{Fj})$ and the filling $n = 2(\pi N)^{-1} \sum k_{Fj}$. Since we are only interested in the low-energy physics, we linearize the dispersion relation around the Fermi momenta, resulting in Fermi velocities $v_j = 2t \sin(k_{Fj})$. We introduce operators $\Psi_{R/Ljs}$ for right- and left movers at the Fermi level in each band.

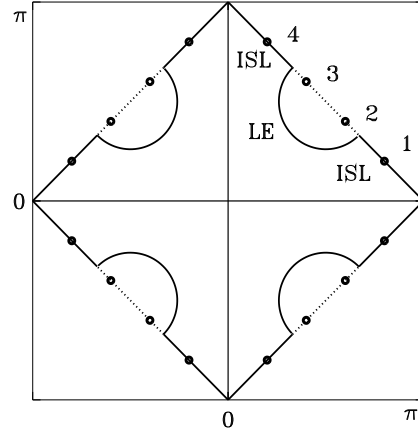


FIG. 2. The bands of the four-leg ladder correspond to four different points on a 2D FS (denoted by 1, 2, 3, and 4). The square is the umklapp surface, which is the FS at half-filling (for $t = t_{\perp}$). The half-circles indicate the opening of the FS, when the bands two and three are doped, forming a Luther-Emery (LE) liquid, where the pairing takes place between quasi-particles at (close to) the wave vectors $(2\pi/5, 3\pi/5)$ and $(3\pi/5, 2\pi/5)$. At $(4\pi/5, \pi/5)$ and $(\pi/5, 4\pi/5)$, the phase is still an ISL. Similarly as for the two-leg ladder, the order-parameter has a different sign in the Fermi points 2 and 3.

At half-filling $n = 1$, $\mu = 0$ and the velocities are given by

$$v_j = v_{\bar{j}} = 2\sqrt{t^2 - \{t_{\perp} \cos[\pi j/(N+1)]\}^2}, \quad (5)$$

where $\bar{j} = N+1-j$. Note that

$$v_1 = v_N < v_2 = v_{N-1} < \dots \quad (6)$$

These particular values of the Fermi velocities will lead to a *hierarchy* of energy scales (see below).

For *generic* Fermi momenta, the interactions are forward- (f) and Cooper- (c) scattering within a band or between two different bands. Following Ref. [14], the interacting part of the Hamiltonian can then be written as

$$H_{\text{Int}} = \sum_{i \neq j} \int dx (f_{ij}^{\rho} J_{Rii} J_{Ljj} - f_{ij}^{\sigma} \mathbf{J}_{Rii} \cdot \mathbf{J}_{Ljj} + c_{ij}^{\rho} J_{Rij} J_{Lij} - c_{ij}^{\sigma} \mathbf{J}_{Rij} \cdot \mathbf{J}_{Lij}) + \sum_j \int dx (c_{jj}^{\rho} J_{Rjj} J_{Ljj} - c_{jj}^{\sigma} \mathbf{J}_{Rjj} \cdot \mathbf{J}_{Ljj}), \quad (7)$$

where the U(1) and SU(2) currents are defined as

$$J_{hij} = \sum_s \Psi_{his}^{\dagger} \Psi_{hjs} \quad (8)$$

and

$$J_{hij}^k = \frac{1}{2} \sum_{s, s'} \Psi_{his}^{\dagger} \tau_{ss'}^k \Psi_{hjs'}, \quad (9)$$

where again $h = R/L$ and the τ^k are the Pauli matrices ($k = x, y, z$). Due to symmetry, $f_{ij}^{\rho, \sigma} = f_{ji}^{\rho, \sigma}$ and $c_{ij}^{\rho, \sigma} = c_{ji}^{\rho, \sigma}$.

In the half-filled case we must generalize the interacting Hamiltonian (7). The Fermi momenta of the bands j and \bar{j} add up to π , $k_{Fj} + k_{F\bar{j}} = \pi$, allowing umklapp interactions to take place between these two bands (for $u_{j\bar{j}jj}^{\rho, \sigma}$ we differ in notation from Ref. [10] by a factor 2),

$$u_{j\bar{j}jj}^{\rho} (I_{Rj\bar{j}}^{\dagger} I_{L\bar{j}j} + \text{H.c.}) - u_{j\bar{j}jj}^{\sigma} (\mathbf{I}_{Rj\bar{j}}^{\dagger} \cdot \mathbf{I}_{L\bar{j}j} + \text{H.c.}) + u_{j\bar{j}jj}^{\rho} (I_{Rjj}^{\dagger} I_{L\bar{j}j} + I_{R\bar{j}j}^{\dagger} I_{Ljj} + \text{H.c.}). \quad (10)$$

We have used the definitions

$$I_{hij} = \sum_{s, s'} \Psi_{his} \epsilon_{ss'} \Psi_{hjs'} \quad (11)$$

and

$$I_{hij}^k = \frac{1}{2} \sum_{s, s'} \Psi_{his} (\epsilon \tau^k)_{ss'} \Psi_{hjs'}, \quad (12)$$

where $\epsilon = -i\tau^y$. For odd N , there exists a single-band umklapp term for the band $r = (N+1)/2$

$$u_{rr}^{\rho} (I_{Rrr}^{\dagger} I_{Lrr} + \text{H.c.}). \quad (13)$$

In addition to these processes, there exist various interactions involving four different bands or three different bands (only for N odd). For the half-filled three-leg ladder, three different three-band umklapp processes

$$\begin{aligned} & u_{1223}^{\rho} (I_{R12}^{\dagger} I_{L23} + I_{R32}^{\dagger} I_{L21} + \text{H.c.}) \\ & + u_{2213}^{\rho} (I_{R22}^{\dagger} I_{L13} + I_{R13}^{\dagger} I_{L22} + \text{H.c.}) \\ & - u_{1223}^{\sigma} (\mathbf{I}_{R12}^{\dagger} \cdot \mathbf{I}_{L23} + \mathbf{I}_{R32}^{\dagger} \cdot \mathbf{I}_{L21} + \text{H.c.}) \end{aligned} \quad (14)$$

and two different three-band non-umklapp processes

$$\begin{aligned} & c_{1223}^{\rho} (J_{R12} J_{L23} + J_{R32} J_{L21} + \text{H.c.}) \\ & - c_{1223}^{\sigma} (\mathbf{J}_{R12} \cdot \mathbf{J}_{L23} + \mathbf{J}_{R32} \cdot \mathbf{J}_{L21} + \text{H.c.}) \end{aligned} \quad (15)$$

take place and have to be added to Eq. (7).

In the four-leg case, the four-band umklapp interactions read

$$\begin{aligned} & u_{1234}^{\rho} (I_{R12}^{\dagger} I_{L34} + I_{R34}^{\dagger} I_{L12} + \text{H.c.}) + u_{1324}^{\rho} (2 \leftrightarrow 3) \\ & + u_{1423}^{\rho} (I_{R14}^{\dagger} I_{L23} + I_{R23}^{\dagger} I_{L14} + \text{H.c.}) \\ & - u_{1234}^{\sigma} (\mathbf{I}_{R12}^{\dagger} \cdot \mathbf{I}_{L34} + \mathbf{I}_{R34}^{\dagger} \cdot \mathbf{I}_{L12} + \text{H.c.}) \\ & - u_{1324}^{\sigma} (2 \leftrightarrow 3) \end{aligned} \quad (16)$$

and the four-band non-umklapp interactions take the form

$$\begin{aligned} & c_{1234}^{\rho} (J_{R12} J_{L34} + J_{R43} J_{L21} + \text{H.c.}) + c_{1324}^{\rho} (2 \leftrightarrow 3) \\ & - c_{1234}^{\sigma} (\mathbf{J}_{R12} \cdot \mathbf{J}_{L34} + \mathbf{J}_{R43} \cdot \mathbf{J}_{L21} + \text{H.c.}) \\ & - c_{1324}^{\sigma} (2 \leftrightarrow 3). \end{aligned} \quad (17)$$

In our case $v_1 = v_4$ and $v_2 = v_3$ implying $c_{1234}^{\rho, \sigma} = c_{1324}^{\rho, \sigma}$, $u_{1234}^{\rho, \sigma} = u_{1324}^{\rho, \sigma}$. The generalization to $N > 4$ is straightforward such that we do not reproduce it here.

The (initial) values of the couplings are of the order of the on-site repulsion U (the exact values are given in Appendix A).

B. Low-energy phases

Using the RG method and bosonization, we derive the low-energy phases. We have generalized the results given in Refs. [10, 14] in order to treat ladders with $N > 2$ legs at half-filling. For weak interactions, $U < t$, it is sufficient to take the RG equations (RGEs) in one-loop order, i.e., quadratic in the coupling constants. For $N = 3$, the full set of RGEs is given in Appendix A (similar RGEs are obtained for $N > 3$ [20]).

The Fermi velocities v_j [see Eqs. (5) and (6)] lead to a hierarchy of energy-scales by $T_j \sim t e^{-\alpha v_j/U}$, where the

band pairs (j, \bar{j}) become successively frozen out. This exponential dependence on v_j/U is a consequence of the logarithmic derivatives of the couplings with respect to the energy in the one-loop RGEs (see Appendix A). As we show below, the low-energy Hamiltonian is then the sum of $N/2$ [$(N-1)/2$ for N odd] two-leg ladder Hamiltonians corresponding to the band pairs (j, \bar{j}) (plus the Hamiltonian of a single chain for N odd).

1. Three-leg ladder

It is instructive to start with the RG flow of the three-leg ladder in the limit $v_1 = v_3 \ll v_2$ (i.e., $t_\perp/t \rightarrow \sqrt{2}$), where we can neglect in the RGEs all contributions, where contractions over the band 2 take place, i.e., the denominator of a term in the RGEs contains at least one v_2 (see Appendix A). We then obtain the following results. First, the renormalization of the two- and single-band interactions of the bands 1 and 3 is exactly the same as for a two-leg ladder, where the couplings flow towards universal ratios (for a comparison, see Ref. [10])

$$\begin{aligned} 0 < 4g_{13} = 4c_{13}^\rho = 4f_{13}^\rho = c_{13}^\sigma = -c_{11}^\sigma = -c_{33}^\sigma \\ &= 4u_{1331}^\rho = 8u_{1133}^\rho = u_{1331}^\sigma, \end{aligned} \quad (18)$$

and

$$c_{11}^\rho = c_{33}^\rho \approx f_{13}^\sigma \approx 0, \quad (19)$$

and become of the order of the bandwidth t at the temperature scale $T_1 \sim te^{-\alpha_1 v_1/U}$ (α_1 is a constant of the order of 1). Second, the interactions between the bands 1 and 2 (and 2 and 3) are either not renormalized or flow to 0. Finally, the scaling of the remaining three-band interactions can be calculated as follows. Defining $\mathbf{v} = (c_{1223}^\rho, c_{1223}^\sigma, u_{1223}^\rho, u_{1223}^\sigma)$ and

$$M = \begin{pmatrix} 2 & 0.75 & 3 & -0.75 \\ 4 & 0 & 4 & -1 \\ 3 & 0.75 & 2 & -0.75 \\ -4 & -1 & -4 & 0 \end{pmatrix}, \quad (20)$$

we obtain the equation (the scaling variable l is related to the energy by $T \sim te^{-\pi l}$)

$$(v_1 + v_3) \frac{d\mathbf{v}}{dl} = g_{13}(l) M \mathbf{v}, \quad (21)$$

where, using Eq. (18), we have expressed the interactions of band 1 and 3 in terms of g_{13} . The eigenvalues of M are $(7, -1, -1, -1)$ and

$$\frac{1}{v_1 + v_3} \int_{l_0}^l g_{13}(l') dl' = \frac{1}{12} \ln \left[\frac{g_{13}(l)}{g_{13}(l_0)} \right], \quad (22)$$

where $l_0 < l$ denotes the scale at which the interactions of the bands 1 and 3 are sufficiently close to the two-leg

ladder ratios. The three-band interactions therefore stay in fixed ratios and

$$\frac{c_{1223}^\rho(l)}{g_{13}(l)} = \frac{c_{1223}^\rho(l_0)}{g_{13}(l_0)} \left[\frac{g_{13}(l_0)}{g_{13}(l)} \right]^{5/12} \propto \left[\frac{U}{g_{13}(l)} \right]^{5/12} \quad (23)$$

such that the three-band interactions are arbitrary small at the scale where $g_{13} \sim t$.

For other ratios of the velocities $v_1/v_2 < 1$, numerical integration of the RGEs shows that the flow of the couplings is still the same as in the limit $v_1 \ll v_2$ (in Ref. [13] a flow to strong coupling of the three-band interactions has been found for $t_\perp/t < 0.86$; we only obtain that for $v_1 \approx v_2$, i.e., in the strongly anisotropic limit $t_\perp/t < 0.2$, which we are not going to consider here).

To conclude our RG analysis of the three-leg ladder: The couplings of the bands 1 and 3 scale towards a two-leg ladder fixed point, become of the order of the bandwidth t at the temperature scale $T_1 \sim te^{-\alpha_1 v_1/U}$, and at (and below) T_1 , the bands 1 and 3 are *decoupled* from the band 2.

Next, using the above RG results, we bosonize the three-leg Hamiltonian (see Appendix B). At the temperature scale T_1 , it is separated in two parts, $H = H_{13} + H_s$. The first term $H_{13} = H_{0,13} + H_{I,13} + H_{u,13}$ is the Hamiltonian of a two-leg ladder (for a comparison, see Ref. [10]), where

$$H_{0,13} = \sum_{j,\nu} \int dx \frac{u_{\nu j}}{2} \left[\frac{1}{K_{\nu j}} (\partial_x \Phi_{\nu j})^2 + K_{\nu j} \Pi_{\nu j}^2 \right], \quad (24)$$

where again the sum goes over the bands $j = 1, 3$ and the charge and spin fields $\nu = \rho, \sigma$. The $H_{I,13}$ includes the non-umklapp interactions, present also away from half-filling (dropping the prefactor),

$$\begin{aligned} H_{I,13} = -g_{13} \int dx &\cos[\beta(\theta_{\rho 1} - \theta_{\rho 3})] \\ &\times \{\cos[\beta(\Phi_{\sigma 1} - \Phi_{\sigma 3})] + \cos[\beta(\Phi_{\sigma 1} + \Phi_{\sigma 3})]\} \\ &+ \cos[\beta(\Phi_{\sigma 1} - \Phi_{\sigma 3})] \cos[\beta(\Phi_{\sigma 1} + \Phi_{\sigma 3})], \end{aligned} \quad (25)$$

where $\beta^2 = 2\pi$, and $H_{u,13}$ results from the umklapp interactions

$$\begin{aligned} H_{u,13} = -g_{13} \int dx &\cos[\beta(\Phi_{\rho 1} + \Phi_{\rho 3})] \{\cos[\beta(\Phi_{\sigma 1} - \Phi_{\sigma 3})] \\ &+ \cos[\beta(\Phi_{\sigma 1} + \Phi_{\sigma 3})] + \cos[\beta(\theta_{\rho 1} - \theta_{\rho 3})]\}. \end{aligned} \quad (26)$$

The second term H_s is the Hamiltonian of a single “chain”,

$$\begin{aligned} H_s = \sum_{\nu=\rho,\sigma} \int dx &\left\{ \frac{u_{\nu s}}{2} \left[\frac{1}{K_{\nu s}} (\partial_x \Phi_{\nu s})^2 + K_{\nu s} \Pi_{\nu s}^2 \right] \right. \\ &\left. - g_{\nu s} \cos(\sqrt{8\pi} \Phi_{\nu s}) \right\}. \end{aligned} \quad (27)$$

The $K_{\nu j}$ are the Luttinger liquid parameters and the $u_{\nu j}$ the velocities of the charge and spin-modes. The coupling

g_{13} is large at the temperature scale T_1 , $g_{13}(T_1) \sim t$ and the various fields become “pinned” (e.g., $\Phi_{\sigma j} \approx 0$) in order to minimize the energy. All the charge and spin-modes of the bands 1 and 3 then acquire a gap. On the contrary, $0 < g_{\nu s} \ll t$, such that at T_1 the charge and spin-modes of band 2 remain gapless.

For a (small but) *finite* U , we then have to investigate the system at energies *below* T_1 . For the Hamiltonian (27) it is well-known that it has a charge gap below a temperature $T_2 \sim te^{-\alpha_2 v_2/U}$ (since $\alpha_2 \approx \alpha_1$ we write in the following α for both of them) and that the spin-excitations remain gapless [19]. Since the two-leg part has no gapless mode, the final phase is C0S1 — the same as for the strongly interacting limit, i.e., a three-leg spin-ladder.

2. Four-leg ladder

For the four-leg ladder, we find a similar behavior. The couplings of the bands 1 and 4 grow, become of the order of the bandwidth t at the energy scale $T_1 \sim te^{-\alpha v_1/U}$, and stay in the same ratio as for a two-leg ladder, while all the other couplings remain small. In the limit $v_1 = v_4 \ll v_2 = v_3$, the RGEs of the four-band couplings become the same as for the three-band couplings and consequently, similarly as above, the four-band interactions stay in fixed ratios and

$$c_{1234}^\rho / c_{14}^\rho \propto (U / c_{14}^\rho)^{5/12}. \quad (28)$$

At the temperature scale T_1 , the bands 1 and 4 are therefore decoupled from the bands 2 and 3. Again, for a finite U , we then have to study the flow of the couplings of band 2 and 3 at energies *below* T_1 . We find that they flow at the scale $T_2 \sim te^{-\alpha v_2/U}$ also to a two-leg ladder fixed point (the flow to the two-leg ladder fixed point takes place for a wide range of initial values, also for non-Hubbard-like). The bosonized Hamiltonian is then the sum of two two-leg ladder Hamiltonians, $H = H_{14} + H_{23}$, where $H_{j\bar{j}}$ has the form of the Hamiltonian given by Eqs. (24), (25) and (26). All charge and spin excitations are therefore gapped (as it is the case in the Heisenberg four-leg spin ladder).

3. The case $N > 4$

Analyzing the RGEs for $N > 4$, we find that this successive freezing out of band pairs (j, \bar{j}) (plus a single band for N odd) at the characteristic energies $T_j \sim te^{-\alpha v_j/U}$ takes place for all finite N with $U \ll t/N$. Again, the T_j are a result of the one-loop RGEs: the couplings of the band pair (j, \bar{j}) scale towards a two-leg ladder fixed point and become of the order of the bandwidth t at T_j . Note that we have a *hierarchy* of energy-scales

$$T_1 > T_2 > \dots > T_r, \quad (29)$$

where for N even $r = N/2$ and for N odd $r = (N+1)/2$.

To conclude this section: At low energies the Hubbard-ladder Hamiltonian becomes for N even the sum of $N/2$ two-leg ladder Hamiltonians and for N odd the sum of $(N-1)/2$ two-leg ladder Hamiltonians plus the Hamiltonian of a single chain

$$H = \sum_j H_{j\bar{j}} + \delta_{N,\text{odd}} H_s, \quad (30)$$

where for N odd, the single chain [the band $(N+1)/2$] has the lowest energy-scale and for N even the two-leg ladder Hamiltonian $H_{N/2,N/2+1}$ [corresponding to the band pair $(N/2, N/2+1)$]. The (half-filled) two-leg ladder Hamiltonians have no gapless excitations and the single-chain Hamiltonian present for odd N has only one gapless spin-mode. The phases at half-filling are thus the same as for the Heisenberg spin-ladders [5]. Since the Hubbard model converges for large U onto the t - J model (which is at half-filling equivalent to the Heisenberg model) [21], the phases of the half-filled N -leg Hubbard ladders are the same for small and large U .

III. HOLE DOPED LADDERS

Since the low-energy cutoff is typically of the order of $te^{-t/U}$, the effect of the umklapp interactions has to be taken into account for low dopings, $\delta < e^{-t/U}$. It is then advantageous to take the *half-filled* ladder as a starting point to study the effect of doping.

In terms of the boson-fields $\Phi_{\rho j}$, the total charge-density is given by $\rho = \partial_x \Phi_\rho$, where $\Phi_\rho = \sum_j \Phi_{\rho j}$ (see Appendix B). At half-filling the energy is minimized by $\Phi_{\rho j} \approx 0$, see Eqs. (26) and (27). An effective Hamiltonian to study the hole doping is therefore obtained by adding a chemical potential term $-\mu \int dx \partial_x \Phi_\rho$ which favors for a sufficiently large μ a nonzero field-configuration with a particular doping (see, e.g., Ref. [10]).

In a single chain, a hole is decomposed in two quasi-particles, one with charge but no spin (holon, here the fermionic “kink”) and the other with spin but no charge (spinon). The quasi-particles of a two-leg ladder are bound hole-pairs (singlet of charge 2). At low doping, these hole-pairs behave as hard-core bosons, which are equivalent to spinless fermions. In Sec. III A, we show that the lightly doped N -leg ladders can indeed be described by an effective $N/2$ -band [$(N+1)/2$ -band for N odd] model of spinless fermions. We then study the case when only one of these bands is doped. In Sec. III B, we increase the hole doping such that many bands become subsequently doped.

A. One band (pair) doped

First, we carry out for the Hamiltonian (30) a canonical transformation to new fields

$$\Phi_{\pm j} = \frac{1}{2} (\Phi_{\rho j} \pm \Phi_{\rho \bar{j}}) \text{ and } \Pi_{\pm j} = \Pi_{\rho j} \pm \Pi_{\rho \bar{j}}. \quad (31)$$

We then integrate out all pinned fields with the exception of Φ_{+j} (and the single chain charge field $\Phi_{\rho s}$), i.e., we replace the fields by their expectation value. Apart from bare energy contributions, we obtain a renormalization of the umklapp couplings. We cast the corresponding contributions in effective couplings g_{+j} . In the quasi-classical frame, this is equivalent to choose for the fields c-numbers, which minimize the energy. In Refs. [10,11], it has been shown that for not too large doping, the spin-gap and the single-particle gap in the two-leg ladder are still present, which justifies this treatment.

Including the chemical potential term, the Hamiltonian (30) takes the form (dropping bare energy terms resulting from Eq. (25))

$$H = \sum_j \int dx \left\{ \frac{u_{+j}}{2} \left[\frac{2}{K_{+j}} (\partial_x \Phi_{+j})^2 + \frac{K_{+j}}{2} \Pi_{+j}^2 \right] - g_{+j} \cos(\sqrt{8\pi} \Phi_{+j}) - 2\mu \partial_x \Phi_{+j} \right\}, \quad (32)$$

plus for odd N the Hamiltonian of a single chain (dropping the gapless spin-part)

$$\int dx \left\{ \frac{u_{\rho s}}{2} \left[\frac{1}{K_{\rho s}} (\partial_x \Phi_{\rho s})^2 + K_{\rho s} \Pi_{\rho s}^2 \right] - g_{\rho s} \cos(\sqrt{8\pi} \Phi_{\rho s}) - \mu \partial_x \Phi_{\rho s} \right\}, \quad (33)$$

where $K_{+j} \rightarrow 1$ and $K_{\rho s} \rightarrow 1/2$ at half-filling [12,19] and the charge (doping) is given by

$$Q = \sqrt{\frac{2}{\pi}} \int dx \sum_j 2\partial_x \Phi_{+j} + \delta_{N, \text{odd}} \partial_x \Phi_{\rho s}. \quad (34)$$

We note that (32) and (33) are the usual Hamiltonians describing a commensurate-incommensurate transition [22]. The fields of the band pair (j, \bar{j}) , Φ_{+j} (and of the single chain $\Phi_{\rho s}$), become pinned at the energy-scales $T_j \sim t e^{-\alpha v_j/U}$. We therefore define effective gaps for the bands by $\Delta_j \sim T_j$, resulting in a hierarchy of gaps (see Eq. (29))

$$\Delta_1 > \Delta_2 > \dots > \Delta_r. \quad (35)$$

The equations of motion following from the Hamiltonians (32) and (33) are a set of sine-Gordon (SG) equations. Here, the physical solutions of the SG equations are the soliton-solutions. Solitons are *fermionic* particles (kinks). The kinks of the single-chain field $\Phi_{\rho s}$ have a

mass $M_s \sim \Delta_s$ and represent the charge part of single holes, while the kinks of the two-leg ladder fields Φ_{+j} have a mass $M_j \sim \Delta_j$ and represent paired holes (singlets). The band structure of these solitons reads

$$\epsilon_j(k) = \sqrt{M_j^2 + (v_j k)^2}. \quad (36)$$

At low doping $\delta < e^{-t/U}$, the half-filled N -leg ladders are therefore described by an effective $N/2$ -band [$(N+1)/2$ -band] model of spinless fermions, where the bottom of the bands are at the energy-scales Δ_j (for $N = 3$, see Fig. 3).

At half-filling, $\mu = 0$ and minimizing the energy gives $\Phi_{+j} \approx \Phi_{\rho s} \approx 0$. When doping the first hole (pair), the chemical potential $\mu = \mu(\delta)$ jumps from 0 to Δ_r and a soliton-solution with charge $Q > 0$ minimizes the energy, i.e., the lowest-lying effective band of spinless fermions becomes doped. For odd N , the lowest-lying band is the single-chain band $(N+1)/2$ and the phase upon doping is a dilute gas of spinons and kinks (C1S1), while for even N , the effective band $N/2$, corresponding to the two-leg-ladder band-pair $(N/2, N/2+1)$, is doped first and the phase consists of singlets of paired holes (C1S0). Similarly as for the two-leg ladder, the (singlet) pair-field operator

$$P_j \propto \Psi_{Rj\uparrow} \Psi_{Lj\downarrow} + \Psi_{Lj\uparrow} \Psi_{Rj\downarrow} \propto \eta_{j\uparrow} \eta_{j\downarrow} \exp(-i\beta\theta_{pj}) \cos(\beta\Phi_{\sigma j}) \quad (37)$$

has a different sign in band j and \bar{j} [10],

$$P_j P_{\bar{j}}^\dagger < 0, \quad (38)$$

such that the C1S0 phase has a d -wave like symmetry.

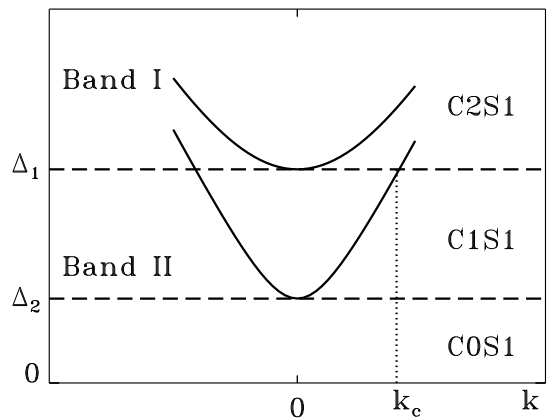


FIG. 3. The lightly doped three-leg ladder can be described by a two-band model of spinless fermions, where the lower band II contains the charge part of holes and the upper band I paired holes (singlets). At half-filling the phase is C0S1; upon doping, the charge part of the holes enters the band II and the phase is C1S1. For dopings $\delta > \delta_c$ (here, $\pi\delta_c = |k_c|$), paired holes enter also the band I and the phase becomes C2S1.

It is instructive to rewrite the band operators Ψ_{hjs} respectively the pair-field operators P_j in terms of the chain operators d_{hjs} . For $N = 3$,

$$\Psi_{h2s} = \frac{1}{\sqrt{2}}(d_{h1s} - d_{h3s}) \quad (39)$$

and we find that the holes are situated on the outer legs. Both the phase and the location of the holes is in agreement with previous numerical treatments [6,7]. For $N = 4$, using $P_2 P_3^\dagger \approx -1$, we obtain

$$\begin{aligned} P_2 \propto & 0.22(d_{R1\uparrow}d_{L2\downarrow} + d_{R2\uparrow}d_{L1\downarrow} + R \leftrightarrow L) \\ & + 0.22(d_{R3\uparrow}d_{L4\downarrow} + d_{R4\uparrow}d_{L3\downarrow} + R \leftrightarrow L) \\ & - 0.36(d_{R1\uparrow}d_{L4\downarrow} + d_{R4\uparrow}d_{L1\downarrow} + R \leftrightarrow L) \\ & - 0.14(d_{R2\uparrow}d_{L3\downarrow} + d_{R3\uparrow}d_{L2\downarrow} + R \leftrightarrow L), \end{aligned} \quad (40)$$

such that the singlets are on the top two legs, the bottom two legs, on the legs 1 and 4, and with lowest probability on the legs 2 and 3, similarly as found in Ref. [4] for the t - J model. Finally, also the phases for $N = 5, 6$ are in agreement with numerical works [4]. Since the t - J model is the large U limit of the Hubbard model [21], we conclude that at and close to half-filling the phases of the N -leg Hubbard ladders are the same for small and large U . For the two-leg ladder, such a “universal” behavior has already been noted in Ref. [12].

B. Many bands doped

When increasing doping, the chemical potential $\mu = \mu(\delta)$ increases too and the hole-pairs enter subsequently also the higher-lying (effective) bands of spinless fermions. We thus obtain a series of critical dopings δ_{cj} , where the first hole-pair enters the band j . For $N = 3, 4$ δ_{c1} is estimated as

$$\delta_{c1} \sim \sqrt{e^{-2\alpha v_1/U} - e^{-2\alpha v_2/U}} \approx e^{-\alpha v_1/U}. \quad (41)$$

Since for $\delta = \delta_{cj}$, $\partial\mu/\partial\delta = 0$, the compressibility

$$\kappa \propto \frac{\partial\delta}{\partial\mu} \quad (42)$$

diverges. The phase transitions at δ_{cj} belong to the same universality class as the commensurate-incommensurate transition [22]. We note that our qualitative estimate for δ_{cj} does not allow for a comparison with numerical works.

The effective band j corresponds to the band pair (j, \bar{j}) , such that for a given doping, the band pairs $(N/2, N/2 + 1), \dots, (j, \bar{j})$ are conducting, while the band pairs $(j - 1, \bar{j} + 1), \dots, (1, N)$ form still an ISL. Next, we interpret this result by mapping each band (pair) on a 2D FS, see Figs. 1 and 2. Using the dispersion relation

(4), the longitudinal Fermi momentum of the band j is given by

$$k_{Fj} = \pi - \arccos\left[\frac{t_\perp}{t} \cos\left(\frac{\pi j}{N+1}\right)\right] \quad (43)$$

and the corresponding transverse Fermi momentum reads

$$k_{Fyj} = \frac{\pi j}{N+1}. \quad (44)$$

Upon doping, the holes enter (for $t_\perp \sim t$) then first near the wave vector $(\pi/2, \pi/2)$ and finally for increasing doping also near $(\pi, 0)$ and $(0, \pi)$. The FS thus becomes truncated, similarly as in the 2D case studied in Ref. [8].

For increasing doping, a crossover takes place to the situation away from half-filling, where the umklapp processes can be neglected. It is instructive to study the phases for $N = 3, 4$, when both effective bands of spinless fermions are doped and to compare with the phase away from half-filling. In the case $N = 3$ (see Fig. 3), the *different charges* in the effective bands I and II *forbid* scattering processes of the form

$$\Psi_{RI}^\dagger \Psi_{RII} \Psi_{LI}^\dagger \Psi_{LII} + I \leftrightarrow II, \quad (45)$$

where $\Psi_{R/Lb}^\dagger$ creates a spinless fermion in band $b = I/II$, since they break $U(1)$ invariance and only the interactions

$$\Psi_{RI}^\dagger \Psi_{RI} \Psi_{LII}^\dagger \Psi_{LII} + I \leftrightarrow II \quad (46)$$

are allowed. For weak interactions, we can bosonize Eq. (46) resulting in a density term of the form $\partial_x \Phi_I \partial_x \Phi_{II}$ (plus the same for the dual fields $\theta_{I,II}$). This term does not reduce the number of gapless modes such that the phase for $\delta > \delta_c$ is C2S1. The same phase has been found by the RG and bosonization methods away from half-filling [13,14]. This contrasts numerical calculations for the strongly interacting t - J model [7], where a spin-gapped phase has been found away from half-filling. Such a phase maybe appears also for weak interactions, if the condensation to the low-energy phase takes place for all bands at the same energy-scale (for another idea, see Ref. [15]).

For $N = 4$, we have two types of paired holes with the same charge in the ladder, localized along the rungs. In contrast to the three-leg case, scattering processes of the form (45) are allowed. We have shown in Ref. [23], that in such a two-band model of spinless fermions with repulsive interactions, slightly away from the band edge, binding takes place and the C2S0 phase close to the band edge becomes C1S0. Away from half-filling, by RG and bosonization, the phase C3S2 has been found [14]. Similarly as already noted in Ref. [15], we argue that the C3S2 phase is a result of the $U \rightarrow 0$ limit considered in Ref. [14]. In contrary, our phases agree with a numerical treatment of the t - J four-leg ladder [16]. At low doping, the authors obtained a phase of paired holes and at

higher doping levels, four-hole clusters (or two-pair clusters). We therefore argue that for increasing doping the phase remains U -independent in even-leg ladders, but not in odd-leg ladders.

We finally note that including next nearest neighbor hopping terms etc., the Fermi momenta of band pairs add up no more exactly to π , i.e., $v_j \approx v_{\bar{j}}$. However, since the phases are controlled by the relative size of gaps, only a *sufficiently large perturbation* can qualitatively change the corresponding physics.

IV. CONCLUSIONS

We have studied the doping away from half-filling in N -leg Hubbard ladders in the case of a small on-site repulsion U , where the ladders are equivalent to a N -band model. At half-filling, the N Fermi velocities are such that $v_1 = v_N < v_2 = v_{N-1} < \dots$. Using RG and bosonization techniques, we have obtained a hierarchy of energy-scales $\Delta_j \sim te^{-\alpha v_j/U}$, where the couplings of the band pair (j, \bar{j}) (and of the single band $(N+1)/2$ for N odd) are of the order of the bandwidth t , decoupled from the other bands, and at a two-leg ladder fixed point. The low-energy Hamiltonian is then the sum of $N/2$ [$(N-1)/2$ for N odd] two-leg ladder Hamiltonians, corresponding to the band pairs (j, \bar{j}) , without gapless excitations (plus for odd N the Hamiltonian of a single chain with one gapless spin-mode). We thus obtain the same phases as for the Heisenberg spin-ladders.

Upon doping, the holes enter first the band (pair) with the smallest gap Δ_j . In odd-leg ladders, this is the nonbonding band $(N+1)/2$ and the phase is a dilute gas of holons (here, the fermionic kinks) and spinons (C1S1), while in even-leg ladders, the band pair $(N/2, N/2+1)$ is doped first and the phase consists of singlets of paired holes (C1S0), reflecting the odd-even effect at half-filling (i.e., of Heisenberg spin-ladders). The same phases have been found in numerical works for the t - J model [4,6,7,16], i.e., at and close to half-filling, the phases of the N -leg Hubbard ladders are the same for small and large U .

For a finite U and at low doping, the ladders can be described by an effective $N/2$ -band model [$(N+1)/2$ -band model for N odd] of spinless fermions, where the (effective) band j corresponds to the band pair (j, \bar{j}) and the bottoms of these bands are at the energy-scales Δ_j . Upon doping, the hole-pairs then subsequently enter these bands and the FS is successively opened, first near the wave vector $(\pi/2, \pi/2)$ and finally also near $(\pi, 0)$ and $(0, \pi)$, similarly as in the 2D case [8]. In addition, we obtain peaks in the compressibility at critical dopings δ_{cj} , where the first hole-pair enters the band pair (j, \bar{j}) .

For increasing doping, the U -independence of the phase seems to break down, at least for odd-leg ladders. However, the U -independence and the similarity to the

2D case at and close to half-filling support the hope that also in 2D, some of the weak-coupling RG results can be extended to large U [8].

ACKNOWLEDGMENTS

We thank S. Haas, C. Honerkamp, and F.C. Zhang for fruitful discussions throughout this work.

APPENDIX A: RENORMALIZATION GROUP

The renormalization group (RG) method is a controlled way of subsequently eliminating (integrating out) high-energy modes in a given Hamiltonian. While the noninteracting part H_0 is at a *RG fixed point*, couplings of the interacting part H_{Int} may grow or decrease under a RG transformation (i.e., when lowering the energy). A subsequent (perturbative) elimination of high-energy modes in H_{Int} then results in RGEs, which give the change of the coupling when lowering the energy, see Ref. [17].

Below, we give the RGEs for the couplings of the three-leg ladder. Using *operator product expansion* for the products of the various currents, the derivation is straightforward [24]. Similar RGEs are obtained in the case $N > 3$ [20].

For the half-filled three-leg ladder $v_1 = v_3$, such that $f_{12}^{\rho, \sigma} = f_{23}^{\rho, \sigma}$, $c_{12}^{\rho, \sigma} = c_{23}^{\rho, \sigma}$, and $c_{11}^{\rho, \sigma} = c_{33}^{\rho, \sigma}$. The initial values of the two and single band couplings are given by

$$f_{13}^{\rho} = c_{11}^{\rho} = c_{13}^{\rho} = \frac{3U}{16}, \quad f_{12}^{\rho} = c_{12}^{\rho} = \frac{U}{8}, \quad c_{22}^{\rho} = \frac{U}{4}, \\ u_{1331}^{\rho} = \frac{3U}{8}, \quad u_{1133}^{\rho} = \frac{3U}{32}, \quad u_{1331}^{\sigma} = 0, \quad u_{22}^{\rho} = \frac{U}{8}, \quad (\text{A1})$$

and $f_{ij}^{\sigma} = 4f_{ij}^{\rho}$, $c_{ij}^{\sigma} = 4c_{ij}^{\rho}$. The initial values of the three-band couplings read

$$c_{1223}^{\rho} = \frac{U}{8}, \quad c_{1223}^{\sigma} = \frac{U}{2}, \\ u_{1223}^{\rho} = \frac{U}{4}, \quad u_{2213}^{\rho} = \frac{U}{8}, \quad u_{1223}^{\sigma} = 0. \quad (\text{A2})$$

The RGEs take the following form, where the energy-scale is related to l by $T \sim te^{-\pi l}$. Starting with the above initial values the RGEs are then numerically integrated up to the scale l_c , where the first coupling is of the order of the bandwidth t . For one-loop RGEs, $l_c = \alpha t/U$, where $\alpha \sim 1$ (this can easily be checked by multiplying the RGEs with t/U^2). We use the abbreviations

$$A_{\pm} = \pm \left[(c_{1223}^{\rho})^2 + \frac{3}{16} (c_{1223}^{\sigma})^2 \right] \\ + (u_{1223}^{\rho})^2 + \frac{3}{16} (u_{1223}^{\sigma})^2$$

$$\begin{aligned}
B_{\pm} &= \pm 4 (c_{1223}^{\rho} c_{1223}^{\sigma} - u_{1223}^{\rho} u_{1223}^{\sigma}) \\
&\quad - (c_{1223}^{\sigma})^2 - (u_{1223}^{\sigma})^2 \\
C_{\pm}^{\rho, \sigma} &= \frac{c_{13}^{\rho, \sigma} + f_{13}^{\rho, \sigma}}{2v_1} \pm \frac{2f_{12}^{\rho, \sigma}}{v_{12}} + \frac{c_{22}^{\rho, \sigma}}{2v_2} \\
D &= c_{1223}^{\rho} u_{1223}^{\rho} - \frac{3}{16} c_{1223}^{\sigma} u_{1223}^{\sigma}, \tag{A3}
\end{aligned}$$

where $v_{12} = v_1 + v_2$.

The two-band forward-scattering interactions are renormalized according

$$\begin{aligned}
\frac{df_{13}^{\rho}}{dl} &= \frac{1}{2v_1} \left[(c_{13}^{\rho})^2 + \frac{3}{16} (c_{13}^{\sigma})^2 + (u_{1331}^{\rho})^2 \right] \\
&\quad + \frac{1}{2v_1} \left[16 (u_{1133}^{\rho})^2 + \frac{3}{16} (u_{1331}^{\sigma})^2 \right] + \frac{A_+}{2v_2} \\
\frac{df_{12}^{\rho}}{dl} &= \frac{1}{v_{12}} \left[(c_{12}^{\rho})^2 + \frac{3}{16} (c_{12}^{\sigma})^2 + 4 (u_{2213}^{\rho})^2 \right] + \frac{A_-}{v_{12}} \\
\frac{df_{13}^{\sigma}}{dl} &= \frac{1}{2v_1} \left[2c_{13}^{\rho} c_{13}^{\sigma} - \frac{1}{2} (c_{13}^{\sigma})^2 - (f_{13}^{\sigma})^2 \right] \\
&\quad + \frac{1}{2v_1} \left[2u_{1331}^{\rho} u_{1331}^{\sigma} - \frac{1}{2} (u_{1331}^{\sigma})^2 \right] + \frac{B_+}{4v_2} \\
\frac{df_{12}^{\sigma}}{dl} &= \frac{1}{v_{12}} \left[2c_{12}^{\rho} c_{12}^{\sigma} - \frac{1}{2} (c_{12}^{\sigma})^2 - (f_{12}^{\sigma})^2 \right] + \frac{B_-}{2v_{12}}, \tag{A4}
\end{aligned}$$

the single-band interactions according

$$\begin{aligned}
\frac{dc_{11}^{\rho}}{dl} &= - \sum_{k \neq 1} \frac{1}{2v_k} \left[(c_{1k}^{\rho})^2 + \frac{3}{16} (c_{1k}^{\sigma})^2 \right] \\
&\quad + \frac{1}{2v_1} \left[(u_{1331}^{\rho})^2 + \frac{3}{16} (u_{1331}^{\sigma})^2 \right] \\
\frac{dc_{22}^{\rho}}{dl} &= - \sum_{k \neq 2} \frac{1}{2v_k} \left[(c_{2k}^{\rho})^2 + \frac{3}{16} (c_{2k}^{\sigma})^2 \right] \\
&\quad + \frac{8}{v_2} (u_{22}^{\rho})^2 + \frac{A_+}{v_1} \\
\frac{dc_{11}^{\sigma}}{dl} &= - \sum_{k \neq 1} \frac{1}{2v_k} \left[\frac{1}{2} (c_{1k}^{\sigma})^2 + 2c_{1k}^{\rho} c_{1k}^{\sigma} \right] - \frac{1}{2v_1} (c_{11}^{\sigma})^2 \\
&\quad - \frac{1}{2v_1} \left[2u_{1331}^{\rho} u_{1331}^{\sigma} + \frac{1}{2} (u_{1331}^{\sigma})^2 \right] \\
\frac{dc_{22}^{\sigma}}{dl} &= - \sum_{k \neq 2} \frac{1}{2v_k} \left[\frac{1}{2} (c_{2k}^{\sigma})^2 + 2c_{2k}^{\rho} c_{2k}^{\sigma} \right] \\
&\quad - \frac{1}{2v_2} (c_{22}^{\sigma})^2 + \frac{B_+}{2v_1}, \tag{A5}
\end{aligned}$$

the two-band back-scattering interactions according

$$\begin{aligned}
\frac{dc_{13}^{\rho}}{dl} &= - \sum_k \frac{1}{2v_k} \left(c_{1k}^{\rho} c_{k3}^{\rho} + \frac{3}{16} c_{1k}^{\sigma} c_{k3}^{\sigma} \right) \\
&\quad + \frac{1}{v_1} \left(c_{13}^{\rho} f_{13}^{\rho} + \frac{3}{16} c_{13}^{\sigma} f_{13}^{\sigma} + 4u_{1133}^{\rho} u_{1331}^{\rho} \right) + \frac{A_+}{2v_2} \\
\frac{dc_{12}^{\rho}}{dl} &= - \sum_k \frac{1}{2v_k} \left(c_{1k}^{\rho} c_{k2}^{\rho} + \frac{3}{16} c_{1k}^{\sigma} c_{k2}^{\sigma} \right)
\end{aligned}$$

$$\begin{aligned}
&\quad + \frac{2}{v_{12}} \left(c_{12}^{\rho} f_{12}^{\rho} + \frac{3}{16} c_{12}^{\sigma} f_{12}^{\sigma} \right) + \frac{4}{v_{12}} u_{2213}^{\rho} u_{1223}^{\rho} \\
\frac{dc_{13}^{\sigma}}{dl} &= - \sum_k \frac{1}{2v_k} \left(c_{1k}^{\rho} c_{k3}^{\sigma} + c_{1k}^{\sigma} c_{k3}^{\rho} + \frac{1}{2} c_{1k}^{\sigma} c_{k3}^{\sigma} \right) + \frac{B_+}{4v_2} \\
&\quad + \frac{1}{v_1} \left(c_{13}^{\rho} f_{13}^{\sigma} + c_{13}^{\sigma} f_{13}^{\rho} - \frac{1}{2} c_{13}^{\sigma} f_{13}^{\sigma} + 4u_{1133}^{\rho} u_{1331}^{\sigma} \right) \\
\frac{dc_{12}^{\sigma}}{dl} &= - \sum_k \frac{1}{2v_k} \left(c_{1k}^{\rho} c_{k2}^{\sigma} + c_{1k}^{\sigma} c_{k2}^{\rho} + \frac{1}{2} c_{1k}^{\sigma} c_{k2}^{\sigma} \right) \\
&\quad + \frac{2}{v_{12}} \left(c_{12}^{\rho} f_{12}^{\sigma} + c_{12}^{\sigma} f_{12}^{\rho} - \frac{1}{2} c_{12}^{\sigma} f_{12}^{\sigma} \right) \\
&\quad + \frac{4}{v_{12}} u_{2213}^{\rho} u_{1223}^{\sigma}, \tag{A6}
\end{aligned}$$

and for the three-band interactions, we find

$$\begin{aligned}
\frac{dc_{1223}^{\rho}}{dl} &= \frac{u_{1331}^{\rho} u_{1223}^{\rho} + 4u_{1133}^{\rho} u_{1223}^{\rho}}{2v_1} - \frac{3u_{1331}^{\sigma} u_{1223}^{\sigma}}{32v_1} \\
&\quad + \frac{2u_{22}^{\rho} u_{1223}^{\rho}}{v_2} + c_{1223}^{\rho} C_{-}^{\rho} + \frac{3c_{1223}^{\sigma} C_{-}^{\sigma}}{16} \\
\frac{dc_{1223}^{\sigma}}{dl} &= - \frac{u_{1223}^{\sigma}}{2v_1} \left(u_{1331}^{\rho} + 4u_{1133}^{\rho} - \frac{1}{2} u_{1331}^{\sigma} \right) \\
&\quad + \frac{u_{1331}^{\sigma} u_{1223}^{\rho}}{2v_1} - \frac{2u_{22}^{\rho} u_{1223}^{\sigma}}{v_2} \\
&\quad + c_{1223}^{\sigma} C_{-}^{\rho} + c_{1223}^{\rho} C_{-}^{\sigma} - \frac{c_{1223}^{\sigma} C_{+}^{\sigma}}{2}, \tag{A7}
\end{aligned}$$

The two- and single-band umklapp interactions are renormalized according

$$\begin{aligned}
\frac{du_{1331}^{\rho}}{dl} &= \frac{u_{1331}^{\rho}}{v_1} (f_{13}^{\rho} + c_{11}^{\rho}) + \frac{3u_{1331}^{\sigma}}{16v_1} (f_{13}^{\sigma} - c_{11}^{\sigma}) \\
&\quad + \frac{4c_{13}^{\rho} u_{1133}^{\rho}}{v_1} + \frac{D}{v_2} \\
\frac{du_{1133}^{\rho}}{dl} &= \frac{c_{13}^{\rho} u_{1331}^{\rho} + 4f_{13}^{\rho} u_{1133}^{\rho}}{2v_1} + \frac{3c_{13}^{\sigma} u_{1331}^{\sigma}}{32v_1} + \frac{D}{2v_2} \\
\frac{du_{1331}^{\sigma}}{dl} &= \frac{u_{1331}^{\rho}}{v_1} (f_{13}^{\sigma} - c_{11}^{\sigma}) + \frac{u_{1331}^{\sigma}}{v_1} (f_{13}^{\rho} + c_{11}^{\rho}) \\
&\quad - \frac{u_{1331}^{\sigma}}{2v_1} (f_{13}^{\sigma} + c_{11}^{\sigma}) + \frac{4c_{13}^{\sigma} u_{1133}^{\rho}}{v_1} \\
&\quad + \frac{1}{2v_2} (c_{1223}^{\sigma} u_{1223}^{\sigma} + 2c_{1223}^{\sigma} u_{1223}^{\rho} - 2c_{1223}^{\rho} u_{1223}^{\sigma}) \\
\frac{du_{22}^{\rho}}{dl} &= \frac{2c_{22}^{\rho} u_{22}^{\rho}}{v_2} + \frac{D}{v_1} \tag{A8}
\end{aligned}$$

and the three-band umklapp interactions according

$$\begin{aligned}
\frac{du_{1223}^{\rho}}{dl} &= \frac{u_{1331}^{\rho} c_{1223}^{\rho} + 4u_{1133}^{\rho} c_{1223}^{\rho}}{2v_1} + \frac{3u_{1331}^{\sigma} c_{1223}^{\sigma}}{32v_1} \\
&\quad + \frac{4u_{2213}^{\rho} c_{12}^{\rho}}{v_{12}} + \frac{2u_{22}^{\rho} c_{1223}^{\rho}}{v_2} \\
&\quad + u_{1223}^{\rho} C_{+}^{\rho} - \frac{3u_{1223}^{\sigma} C_{-}^{\sigma}}{16}
\end{aligned}$$

$$\begin{aligned}
\frac{du_{2213}^\rho}{dl} &= \frac{2u_{1223}^\rho c_{12}^\rho}{v_{12}} + \frac{3u_{1223}^\sigma c_{12}^\sigma}{8v_{12}} + \frac{4u_{2213}^\rho f_{12}^\rho}{v_{12}} \\
\frac{du_{1223}^\sigma}{dl} &= -\frac{c_{1223}^\sigma}{2v_1} \left(u_{1331}^\rho + 4u_{1133}^\rho - \frac{1}{2}u_{1331}^\sigma \right) \\
&\quad - \frac{u_{1331}^\sigma c_{1223}^\rho}{2v_1} + \frac{4u_{2213}^\rho c_{12}^\sigma}{v_{12}} - \frac{2u_{22}^\rho c_{1223}^\sigma}{v_2} \\
&\quad - u_{1223}^\rho C_-^\sigma + u_{1223}^\sigma C_+^\rho - \frac{u_{1223}^\sigma}{2} C_+^\sigma. \tag{A9}
\end{aligned}$$

APPENDIX B: BOSONIZATION

The method of rewriting fermionic creation (annihilation) operators in terms of field operators Φ and Π satisfying the commutation relation

$$[\Phi(x), \Pi(y)] = i\delta(x - y), \tag{B1}$$

is called *bosonization*. For fermions on a chain or ladder, bosonization applies in the *continuum limit*.

It is convenient to introduce the dual field of Φ ,

$$\theta(x) = \int_{-\infty}^x dx' \Pi(x'). \tag{B2}$$

For spin-1/2 fermions, the bosonization scheme is then as follows (see, e.g., Refs. [18,19]). Fermionic operators Ψ_{hs} ($h = R/L$) transform according

$$\Psi_{hs} = \frac{\eta_s}{\sqrt{2\pi a}} \exp \left\{ i\sqrt{\pi/2} [\pm(\Phi_\rho + s\Phi_\sigma) - (\theta_\rho + s\theta_\sigma)] \right\}, \tag{B3}$$

where a is a cutoff parameter of the order of the lattice constant and the η_s are Majorana (“real”) fermionic operators (usually called “Klein factors”) which are necessary to fulfill the anticommutation relations. The U(1) symmetric “charge currents”

$$J_h = \sum_s \Psi_{hs}^\dagger \Psi_{hs}, \tag{B4}$$

take the form

$$J_L + J_R = \sqrt{\frac{2}{\pi}} \partial_x \Phi_\rho \quad \text{and} \quad J_L - J_R = \sqrt{\frac{2}{\pi}} \Pi_\rho \tag{B5}$$

and the z -component of the SU(2) symmetric “spin currents”

$$J_h^k = \frac{1}{2} \sum_{s,s'} \Psi_{hs}^\dagger \tau_{ss'}^k \Psi_{hs'}, \tag{B6}$$

where the τ^k are the Pauli matrices, becomes

$$J_L^z + J_R^z = \frac{1}{\sqrt{2\pi}} \partial_x \Phi_\sigma \quad \text{and} \quad J_L^z - J_R^z = \frac{1}{\sqrt{2\pi}} \Pi_\sigma. \tag{B7}$$

Here, we apply bosonization on the N band operators Ψ_{hjs} . For the Klein factors, we choose the “gauge”

$$\eta_{j\uparrow} \eta_{j\downarrow} \eta_{\bar{j}\uparrow} \eta_{\bar{j}\downarrow} = 1. \tag{B8}$$

Using the above rules it is then straightforward to obtain the bosonized Hamiltonians (24), (25), (26), and (27), where we have dropped the factor $1/(2\pi a)^2$.

- [1] E. Dagotto, J. Riera, and D.J. Scalapino, Phys. Rev. B **45**, 5744 (1992).
- [2] T.M. Rice, S. Gopalan, and M. Sigrist, Europhys. Lett. **23**, 445 (1993).
- [3] M. Uehara, T. Nagata, J. Akimitsu, H. Takahashi, N. Mori, and K. Kinoshita, J. Phys. Soc. Jpn **65**, 2764 (1996).
- [4] S.R. White and D.J. Scalapino, Phys. Rev. B **55**, 6504 (1997).
- [5] E. Dagotto and T.M. Rice, Science **271**, 618 (1996).
- [6] T.M. Rice, S. Haas, M. Sigrist, and F.C. Zhang, Phys. Rev. B **56**, 14655 (1997).
- [7] S.R. White and D.J. Scalapino, Phys. Rev. B **57**, 3031 (1998).
- [8] N. Furukawa, T.M. Rice, and M. Salmhofer, Phys. Rev. Lett. **81**, 3195 (1998); C. Honerkamp, M. Salmhofer, N. Furukawa, and T.M. Rice, cond-mat/9912358.
- [9] M. Fabrizio, Phys. Rev. B **48**, 15838 (1993); D.V. Khveshchenko and T.M. Rice, Phys. Rev. B **50**, 252 (1994); H.J. Schulz, Phys. Rev. B **53**, R2959 (1996); L. Balents and M. Fisher, Phys. Rev. B **53**, 12133 (1996).
- [10] H. Lin, L. Balents, and M. Fisher, Phys. Rev. B **58**, 1794 (1998).
- [11] R. Konik *et al.*, cond-mat/9806334; R. Konik and A.W.W. Ludwig, cond-mat/9810332.
- [12] H.J. Schulz, Phys. Rev. B **59**, R2471 (1999).
- [13] E. Arrigoni, Phys. Lett. A **215**, 91 (1996).
- [14] H. Lin, L. Balents, and M. Fisher, Phys. Rev. B **56**, 6569 (1997).
- [15] V.J. Emery, S.A. Kivelson, and O. Zachar, Phys. Rev. B **56**, 6120 (1997) and Phys. Rev. B **59**, 15641 (1999).
- [16] S.R. White and D.J. Scalapino, Phys. Rev. B **55**, R14701 (1997).
- [17] R. Shankar, Rev. Mod. Phys. **66**, 129 (1994).
- [18] F.D.M. Haldane, J. Phys. C **14**, 2585 (1981).
- [19] H.J. Schulz, in *Proceedings of Les Houches Summer School LXI*, edited by E. Akkermans *et al.* (Elsevier, Amsterdam, 1995).
- [20] U. Ledermann, (unpublished).
- [21] C. Gros, R. Joynt, and T.M. Rice, Phys. Rev. B **36**, 381 (1987).
- [22] G.I. Dzhaparidze and A.A. Nersesyan, JETP Lett. **27**, 334 (1978); V.L. Pokrovsky and A.L. Talapov, Phys. Rev. Lett. **42**, 65 (1979); H.J. Schulz, Phys. Rev. B **22**, 5274 (1980).
- [23] U. Ledermann and K. Le Hur, Phys. Rev. B **61**, 2497 (2000).
- [24] A.W.W. Ludwig, in *Quantum Field Theory and Condensed Matter Physics; Proceedings of the Fourth Trieste Conference, Trieste, Italy, 1991*, edited by S. Randjbar-Daemi and Yu Lu (World Scientific, Singapore, 1994).